Clinical evaluation of time-resolved spectroscopy by measuring cerebral hemodynamics during cardiopulmonary bypass surgery

Etsuko Ohmae
Motoki Oda
Toshihiko Suzuki
Yutaka Yamashita
Hamamatsu Photonics K.K.
Central Research Laboratory
5000 Hirakuchi, Hamamatsu
Shizuoka, 434-8601, Japan

Yasuyuki Kakihana
Kagoshima University Hospital
Division of Intensive Care Medicine
8-35-1 Sakuragaoka
Kagoshima, 890-8520, Japan

Akira Matsunaga
Yuichi Kanmura
Kagoshima University School of Medicine
Division of Anesthesiology and Critical Care Medicine
8-35-1, Sakuragaoka
Kagoshima, 890-8544, Japan

Mamoru Tamura
Hokkaido University
Faculty of Advanced Life Science
Division of Biophysics
N12 W6, Kita-Ku
Sapporo, 060-0812, Japan

Abstract. We developed a three-wavelength time-resolved spectroscopy (TRS) system, which allows quantitative measurement of hemodynamics within relatively large living tissue. We clinically evaluated this TRS system by monitoring cerebral circulation during cardiopulmonary bypass surgery. Oxyhemoglobin, deoxyhemoglobin, total hemoglobin and oxygen saturation (SO_2) were determined by TRS on the left forehead attached with an optode spacing of 4 cm. We also simultaneously monitored jugular venous oxygen saturation ($SjvO_2$) and arterial blood hematocrit (Hct) using conventional methods. The validity and usefulness of the TRS system were assessed by comparing parameters obtained with the TRS and conventional methods. Although the changes in SO_2 were lower than those in $SjvO_2$, SO_2 obtained by TRS paralleled the fluctuations in $SjvO_2$, and a good correlation between these values was observed. The only exceptions occurred during the perfusion period. Moreover, there was a good correlation between tHb and Hct values ($r^2=0.63$). We concluded that time-resolved spectroscopy reflected the conditions of cerebral hemodynamics of patients during surgical operations. [DOI: 10.1117/1.2804931]

Keywords: near-infrared spectroscopy (NIRS); time-resolved spectroscopy (TRS); cardiopulmonary bypass; jugular venous oxygen saturation ($SjvO_2$).

Paper 07083SSR received Mar. 1, 2007; revised manuscript received Aug. 8, 2007; accepted for publication Aug. 15, 2007; published online Nov. 15, 2007.

1 Introduction

Near-infrared spectroscopy (NIRS) at a wavelength between 700 and 900 nm is useful for continuously and noninvasively assessing the oxygenation state *in vivo*. This method is based on the relatively high tissue transparency of near-infrared light in addition to hemoglobin absorption in the region. There are many reports on the clinical applications of NIRS, such as monitoring cerebral oxygen metabolism during surgery[1,2] or for the respiratory management of neonates.[3,4] In particular, it may prove useful to monitoring cerebral circulation during cardiac surgery under extracorporeal circulation, which is associated with high risks of cerebral ischemia, embolism, hyperperfusion after release from the artificial heart-lung machine, and cerebral complications such as postoperative deterioration of neural recognition.[5,6] Commercially available NIRS monitors have been used for comparing oxygen saturation (SO_2) with internal jugular vein oxygen saturation ($SjvO_2$)[7–14] or electroencephalographs[15–17] and for assessing changes in blood volume.[18]

Address all correspondence to Etsuko Ohmae, Hamamatsu Photonics K.K., Central Research Laboratory, 5000 Hirakuchi, Hamamatsu, Shizuoka, 434-8601, Japan; Tel: +81-53-586-7111; Fax: +81-53-586-6180; E-mail: etuko-o@crl.hpk.co.jp

However, the NIRS apparatus used employs continuous wave (CW) near-infrared light. Therefore, absolute values of hemoglobin concentration and highly reproducible SO_2 cannot be obtained. To overcome these difficulties, more sophisticated technologies have been introduced.

Phase modulation spectroscopy (PMS)[19–23] and time-resolved spectroscopy (TRS)[24–27] have been developed for this purpose. However, these new technologies have not been evaluated in detail in a clinical study.[28]

In TRS, the distribution of optical path lengths is directly measured. Its temporal profile is analyzed using a photon diffusion equation[25] and the Microscopic Beer-Lambert law,[29] thereby enabling determination of the hemoglobin concentration.

Our three-wavelength time-resolved spectroscopy system (TRS-10)[30] was tested in cardiopulmonary bypass surgery, during which the absolute concentrations of oxygenated, deoxygenated, and total hemoglobin were estimated. SO_2 was simultaneously calculated as a percentage of oxygenated hemoglobin of total hemoglobin. The optically estimated values were compared with those of $SjvO_2$ and hematocrit (Hct) in

1083-3668/2007/12(6)/062112/9/$25.00 © 2007 SPIE

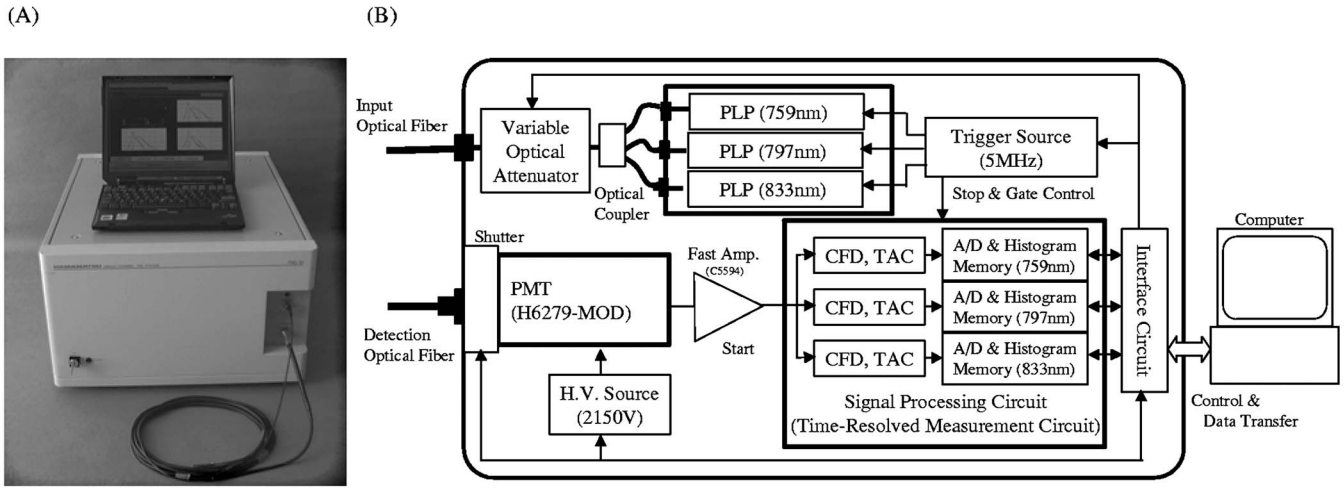

Fig. 1 (a) Appearance of TRS-10 (Hamamatsu Photonics K.K.). (b) Block diagram of the TRS-10 system.

arterial blood. The validity and usefulness of our optical measurements are demonstrated in this clinical study.

2 Materials and Methods

2.1 *Experimental Procedure*

Twenty-three patients (mean age 63.4±12.3; 15 men, 8 women) who underwent coronary-artery bypass surgery in Kagoshima University Hospital were subjected to the study. Before surgery, blood was drawn in installments. Body temperature was controlled to achieve a mild hypothermic condition (32°C) using α-stat regulation.

After anesthesia, the optical probes connected to the time-resolved spectroscopy system (TRS-10) were attached to the left forehead with an optode distance of 4 cm. Each sampling time was 10 s, and HbO_2, Hb, tHb, and SO_2 were continuously measured for 5 min (resting conditions). In 9 of the 23 patients (mean age 65.00±9.4; 8 men, 1 woman), the TRS measurements were continued until the surgery was completed. Arterial blood was collected from those patients during surgery, through a 20-gauge catheter placed in the radial artery. Their Hct values were determined from the arterial hemoglobin concentration (Hg) by blood gas analysis (ABL 2; Radiometer, Copenhagen, Denmark) as follows:

$$Hct = \frac{Hg}{MCHC} = Hg \times 0.0301 \times 100, \qquad (1)$$

where *Hct* is the hematocrit [%], *Hg* is the arterial hemoglobin concentration [g/dl], and *MCHC* is the mean corpuscular hemoglobin concentration [g/L]; the standard value is 332.

In 6 of the 9 patients (mean age 64.5±6.5; 5 men, 1 woman), $SjvO_2$ was also measured using a 5.5 Fr Opticathe (Abbott Critical Care Systems, Mountain View, California) that was regressively placed in the left internal jugular vein bulb.

2.2 *Time-Resolved Spectroscopy System (TRS-10)*

Our time-resolved spectroscopy system (TRS-10) uses the time-correlated single photon counting (TCPC) method to measure the temporal profile of the detected photons, as shown in Fig. 1. The apparatus is described elsewhere.[30]

In brief, the system consists of a three-wavelength (759 nm, 797 nm, and 833 nm) light pulser (PLP, Hamamatsu Photonics K.K., Hamamatsu, Japan) as the light source, which generates light pulses with a peak power of 60 mW, pulse width of 100 ps, pulse rate of 5 MHz, and an average power of 30 μW. For the detection, a photomultiplier tube (PMT, H6279-MOD, Hamamatsu Photonics K.K.), a constant fraction discriminator (CFD), a time-to-amplitude converter (TAC), an A/D converter, and a histogram memory were all assembled. The three PLPs emit light pulses on a time series, and three-wavelength light pulses are guided into one illuminating optical fiber by a fiber coupler (CH20G-D3-CF, Mitsubishi Gas Chemical Company, Inc., Japan). A single optical fiber (GC200/250L, Fujikura Ltd., Japan) with a numerical aperture (N.A.) of 0.21 and a core diameter of 200 μm was used for illumination. An optical bundle fiber (LB21E, Moritex Corporation, Japan) with an N.A. of 0.21 and a bundle diameter of 3 mm was used to collect diffuse light from the tissues.

2.3 *Data Analysis*

TRS allows the determination of relative light intensity, mean optical path length, scattering coefficient (μ_s'), and absorption coefficient (μ_a).

The intensity can be obtained by integrating the temporal profiles and modified Beer-Lambert law (MBL) uses this information to calculate the absorbance changes. The mean optical path lengths were calculated from the center of gravity of the temporal profile.[31]

Applying the diffusion equation for semi-infinite homogeneous media with zero boundary condition in reflectance mode[25] into all the observed temporal profiles, we obtained the values of μ_s' and μ_a using the nonlinear least-squares method.[32]

We first assumed that absorption in the 700 to 900 nm range arises from oxygenated hemoglobin (HbO_2), deoxygenated hemoglobin (Hb), and water. The contributions of myo-

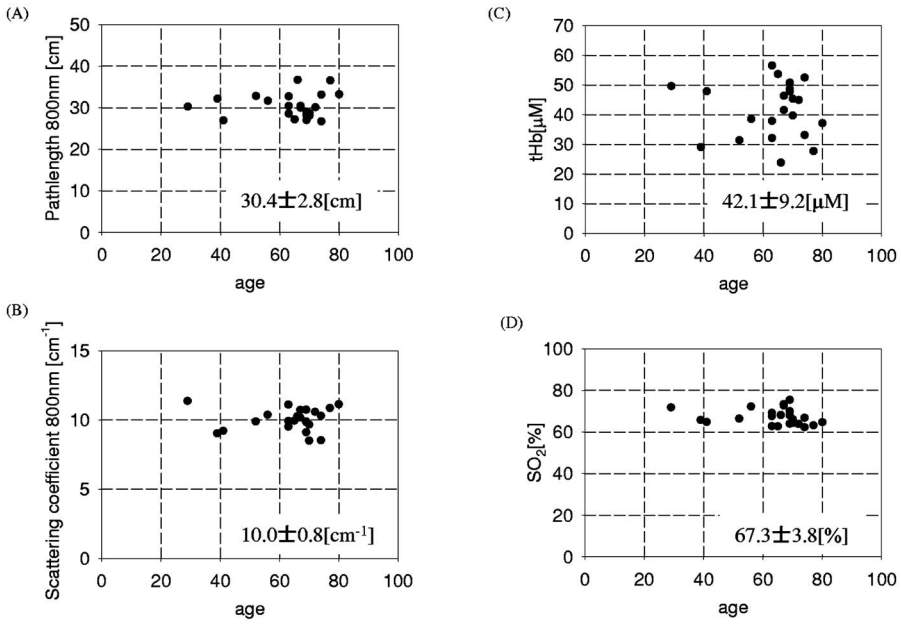

Fig. 2 The variations of (a) mean optical path length, (b) μ_s', (c) tHb, and (d) SO_2 in 23 patients under resting conditions are plotted against age.

globin and cytochrome oxidase could be ignored. The $\mu_{a\lambda}$ of the measured wavelengths λ (759, 797, and 833 nm) is expressed as shown in simultaneous Eq. (2):

$$\mu_{a759nm} = \varepsilon_{HbO_2 759\ \mathrm{nm}} C_{HbO_2} + \varepsilon_{Hb759\ \mathrm{nm}} C_{Hb} + \mu_{aH_2O759\ \mathrm{nm}},$$

$$\mu_{a797nm} = \varepsilon_{HbO_2 797\ \mathrm{nm}} C_{HbO_2} + \varepsilon_{Hb797\ \mathrm{nm}} C_{Hb} + \mu_{aH_2O797\ \mathrm{nm}},$$

$$\mu_{a833nm} = \varepsilon_{HbO_2 833\ \mathrm{nm}} C_{HbO_2} + \varepsilon_{Hb833\ \mathrm{nm}} C_{Hb} + \mu_{aH_2O833\ \mathrm{nm}}, \tag{2}$$

where $\varepsilon_{m\lambda}$ is the molar extinction coefficient of substance m at wavelength λ, and C_m is the concentration of substance m. The water absorption ($\mu_{aH_2O\lambda}$) was measured using a conventional spectral photometer (U-3500, Hitachi High-Technologies Corporation).

After subtracting the water absorption from μ_a at each wavelength assuming that volume fraction of the water content was constant,[33] we determined the concentrations of HbO_2 and Hb using the least-squares fitting method.

The total concentrations of hemoglobin (tHb) and oxygen saturation (SO_2) were calculated from Eqs. (3) and (4):

$$tHb = HbO_2 + Hb, \tag{3}$$

$$SO_2 = \frac{HbO_2}{tHb} \times 100. \tag{4}$$

2.4 *Statistical Analysis*

All the numerical data are presented as the mean value ± standard deviation (SD). The correlation of SO_2 and $SjvO_2$ was evaluated with Pearson's correlation coefficient. The Bland-Altman test was also used to study the agreement between SO_2 and $SjvO_2$. The precision of the bias estimate was defined as 2 SD of the mean difference. The correlation of Hct and tHb was evaluated with Pearson's correlation coefficient, assuming that the cerebral blood volume is constant during surgery.

3 Results

The variations of mean optical path length, μ_s', tHb, and SO_2 in 23 patients under resting conditions are plotted against age, as shown in Fig. 2. The mean optical path length was 30.4±2.8 cm, μ_s' was 10.0±0.8 cm^{-1}, tHb was 42.1±9.2 μM, and SO_2 was 67.3±3.8%. SO_2 varied the least among the patients, while the tHb varied significantly.

Figure 3 shows a typical case (Case 4, F, 63Y) of photon count rates (light intensity), mean optical path lengths, μ_s', and μ_a at three wavelengths during coronary-artery bypass surgery. These values (except μ_s') changed significantly due to hemodilution during extracorporeal circulation.

Figure 4 shows the relationship between the TRS parameters (μ_a, μ_s', and the mean optical path length at three wavelengths) and the Hct value of arterial blood collected during surgery in a typical case (Case 4, F, 63Y). In this patient, the Hct value at the beginning of surgery was 23% but decreased to a minimum of 12% during extracorporeal circulation. μ_a changed linearly in relation to Hct changes, while μ_s' remained almost unchanged. The mean optical path length increased with the decrease of Hct.

Figure 5(a) shows the time course of changes in the concentration of HbO_2, Hb, and tHb, and the SO_2 and $SjvO_2$ are shown in Fig. 5(b). When extracorporeal circulation was started, HbO_2 and tHb decreased abruptly, together with decreases in SO_2. After the release of extracorporeal circulation, those values returned to the initial levels.

The SO_2 estimated by TRS was nearly the same as that of $SjvO_2$ before extracorporeal circulation, but during circula-

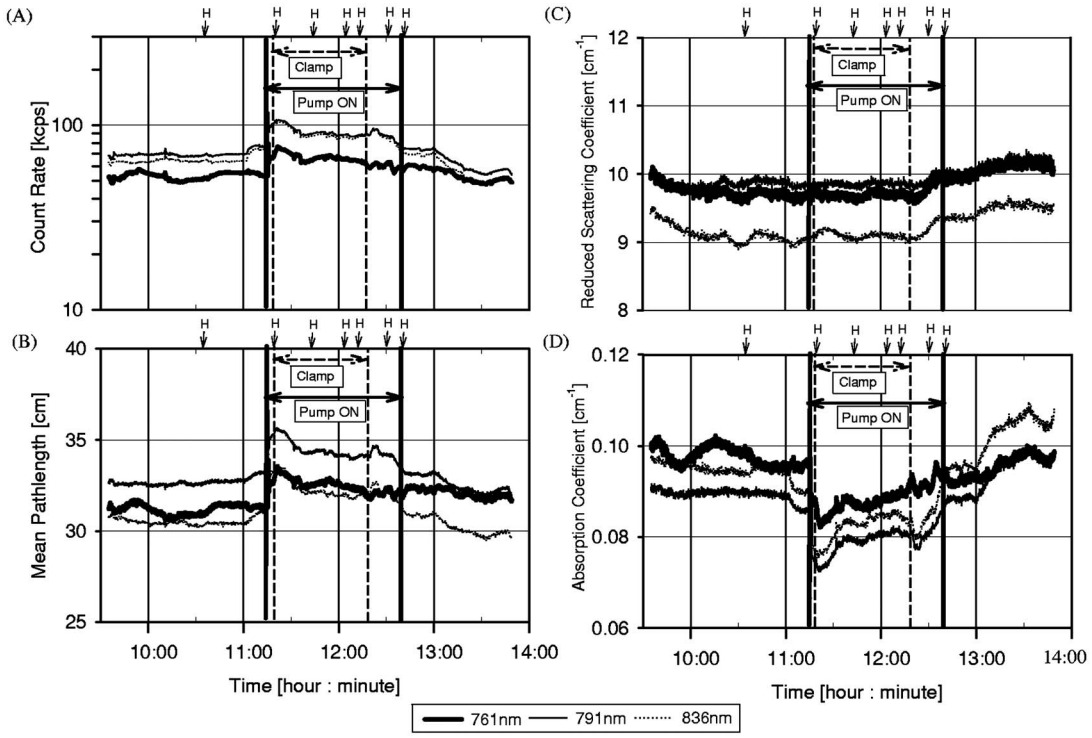

Fig. 3 Time course of TRS-10 parameters during surgery in a typical case (Case 4: F, 63Y): (a) count rate, (b) mean optical path length, (c) μ_s', and (d) μ_a. H: drawing arterial blood to determine hematocrit (Hct).

tion, they behaved differently. Especially when rewarming was carried out, SO_2 did not vary as much as $SjvO_2$.

Figure 6 shows that fluctuations in SO_2 and $SjvO_2$ were separated during extracorporeal circulation in one case (Case 3, M, 52Y). The values of $SjvO_2$ increased significantly when the pump was on, whereas SO_2 decreased rapidly.

Figure 7 shows the correlation between the Hct in arterial blood and tHb in nine patients. The correlation among patients was high, with $r^2=0.63$, showing that tHb measured by TRS has a good linearity with Hct. In addition, intraindividual correlations were also very high ($r^2=0.72\pm0.22$; data is not shown).

Figure 8 shows the linear regression plot and the Bland-Altman plot of SO_2 and $SjvO_2$ for all data of six patients: during the whole surgery (a), during the surgery except perfusion (b), during partial perfusion (c), and during total perfusion (d). The correlation coefficients were $r^2=0.33$ in (a), $r^2=0.46$ in (b), $r^2=0.29$ in (c), and $r^2=0.42$ in (d). The bias and the precision (±2 SD) were 0.66±19.6% in (a), 2.90±18.7% in (b), 0.92±16.5% in (c), and −5.21±17.9% in (d). The correlation coefficient in (c) and bias in (d) were lower than those in other stages of the operation. This variation was split into inter- and intraindividual analysis, and the results of correlation, bias, and precision among six patients

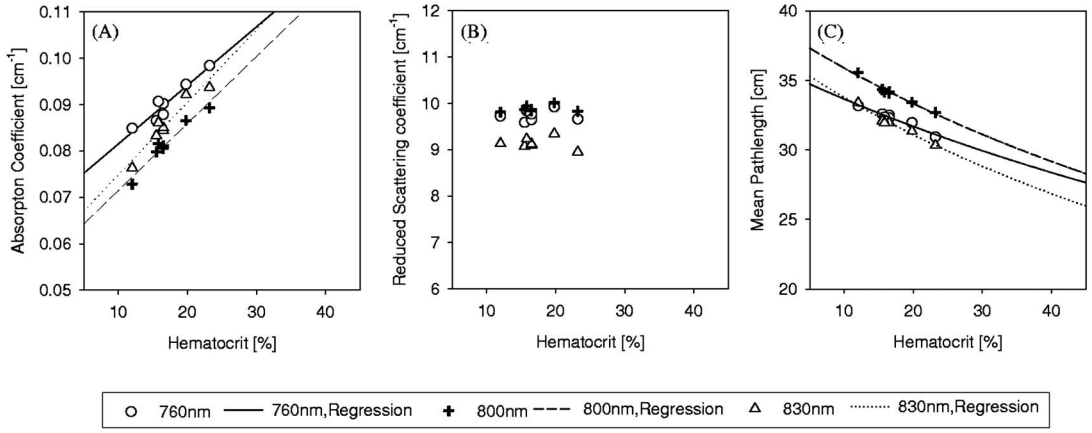

Fig. 4 Relationship TRS parameters at three wavelengths and hematocrit (Hct) value in the typical case (Case 4: F, 63Y): (a) μ_a, (b) μ_s', and (c) mean optical path length.

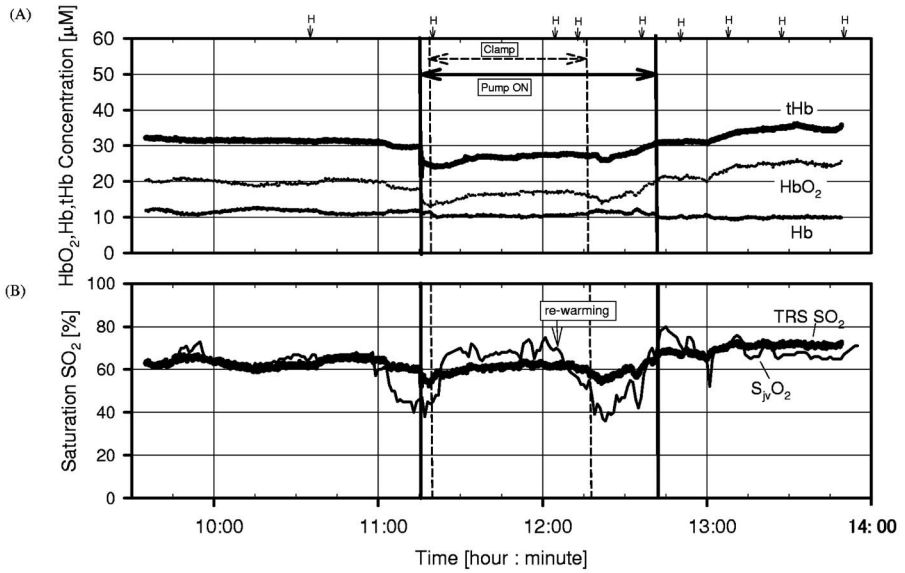

Fig. 5 Hemoglobin concentrations and SO_2 as measured by TRS-10 during surgery in the typical case (Case 4: F, 63Y): (a) HbO_2, Hb, and tHb; (b) TRS SO_2, $SjvO_2$. H: in arterial blood drawn to determine Hct.

and the mean of these values within six patients are shown in Table 1. Precisions become smaller for intraindividual analysis, although biases did not show such changes.

Figure 9(a) shows the plot of the μ_s' during the surgery in one patient (Case 5, M, 69Y). The μ_s' decreased gradually during perfusion only in this case. The other eight patients did not show such changes of μ_s' during surgery [Fig. 9(b), Case 7, M, 66Y].

4 Discussion

In the present study, the observed values of tHb showed wide variation in resting conditions, reflecting different preoperative blood drawing for each patient. In contrast, SO_2 in resting conditions was very similar among patients. This parameter, which is independent of patient age and Hct, is very useful for monitoring the brain tissue oxygenation of each patient.

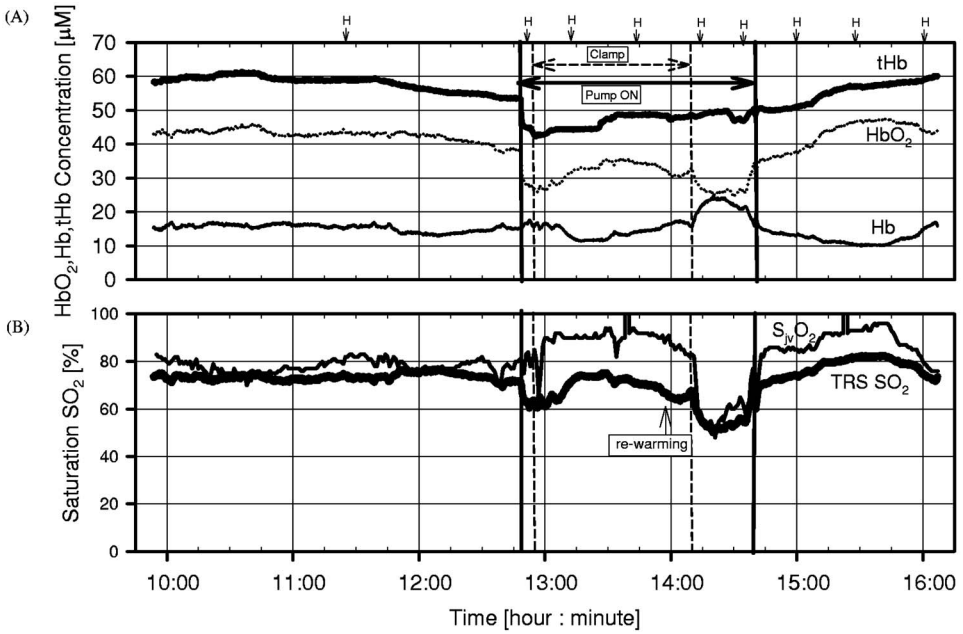

Fig. 6 Fluctuations of SO_2 and $SjvO_2$ were separated during extracorporeal circulation in one patient (Case 3: M, 52Y). When the pump was on, the values of $SjvO_2$ increased significantly. Meanwhile, those of SO_2 decreased rapidly. (a) HbO_2, Hb, and tHb; (b) TRS SO_2, $SjvO_2$. H: in arterial blood drawn to determine Hct.

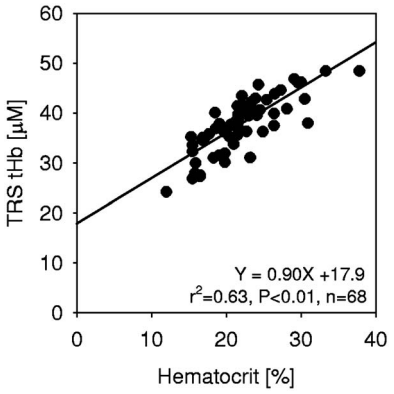

Fig. 7 Relationship between tHb by TRS-10 and hematocrit (Hct) in nine patients.

During surgery under extracorporeal circulation, the Hct value decreased further due to hemodilution to prevent the formation of thrombi. The various parameters (count rate, mean optical path length, μ_a) determined by TRS and tHb responded well to changes in such hemodilution as shown in Figs. 3 and 4. In particular, μ_a varied linearly with Hct. Although several conventional approaches use CW-methods that assume a constant value of the mean optical path length in the calculation, it should be noted that there are large fluctuations among the patients. Thus, the quantitative measurements employed here are necessary to continuously monitor the condition of patients during the operation. Although μ_a and the mean optical path length were affected by Hct changes, μ_s' showed almost constant values without being affected by Hct changes. This result supports the proposition that absorption and scattering can be handled independently.

In this study, we observed the decrease of μ_s' during perfusion in one patient, as shown in Fig. 9(a). The trend of HbO_2, Hb, tHb, and SO_2 were not much different from other cases. System drift was significantly smaller than the change in μ_s' of the patient. The chief contributor to the scattering of tissues is their organelle contents such as mitochondria, endoplasmic reticulum, nucleus, and so forth.[34] There are reports on the relationship between the μ_s' and the developmental stages of a newborn baby's brain.[35] Moreover, change in μ_s' of a piglet brain caused by the depolarization has been demonstrated when the piglets were exposed to hypoxia.[27,36] The possibility of inducing scattering changes by almost any kind of solute (particularly glucose, mannitol, and sucrose) has been suggested.[34] Although more research is necessary for ascertaining the clinical implications of scattering change, it has been reported that such information is important.[27,34–36] It may be used to prevent risks leading to brain damage, such as cerebral edema.

We have demonstrated the usefulness of our TRS system for monitoring the state of brain oxygenation, as well as tissue optical parameters related to physiological conditions of cerebral tissue. The TRS allows the quantification of HbO_2, Hb, and tHb of the brain. Both correlations between Hct and tHb within patients and among patients were high, even though the anatomical structure such as the thicknesses of the scalp and skull might be different in individuals. The effect of the outer layer may be smaller in time-resolved spectroscopy than that of the conventional CW method.[37,38]

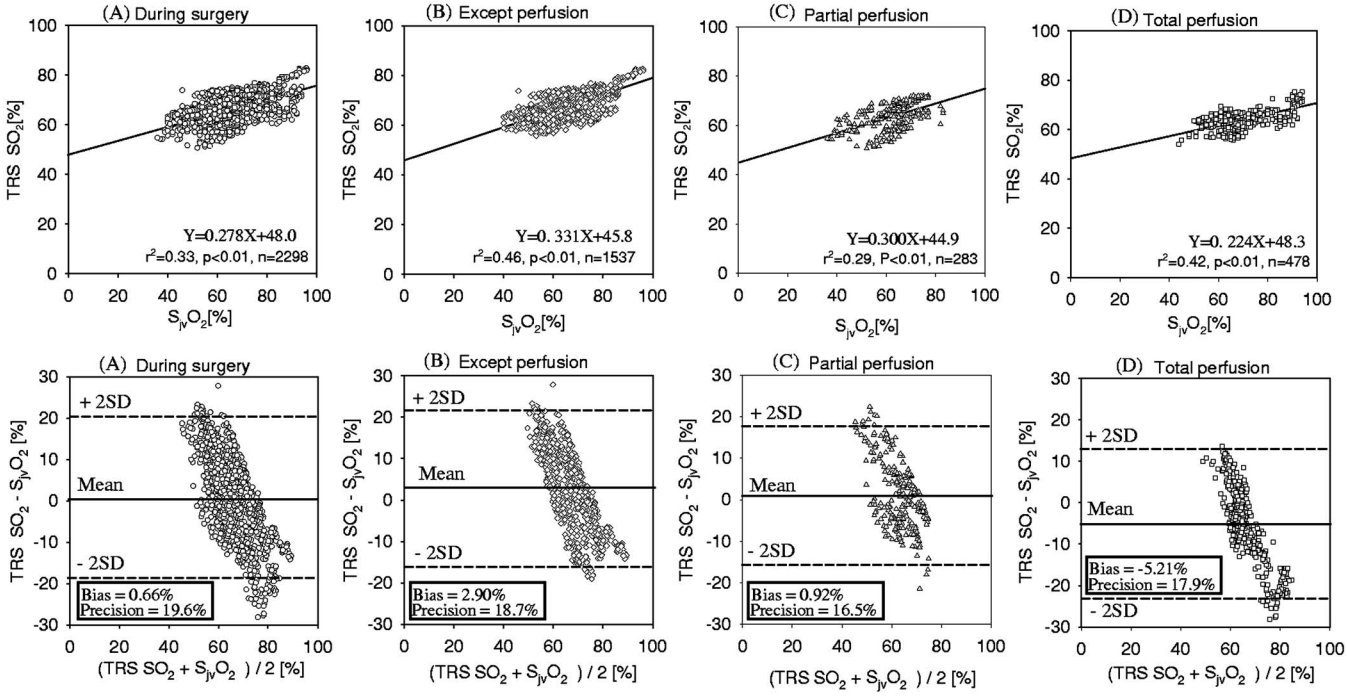

Fig. 8 Linear regression correlation between SO_2 and $SjvO_2$ (upper) and difference plots for SO_2 and $SjvO_2$ using the Bland-Altman method (lower) in all data points of six patients: (a) during the whole surgery, (b) during the surgery except perfusion, (c) during partial perfusion, and (d) during total perfusion.

Table 1 The correlation and agreement between SO_2 and $SjvO_2$.

	Mean for each patient ($n=6$)			All individual values		
	r^2	Bias	Precision	r^2	Bias	Precision
(a) During surgery	0.23	1.29	±14.72	0.33	0.66	±19.6
(b) Except perfusion	0.47	3.52	±12.35	0.46	2.90	±18.7
(c) Partial perfusion	0.41	2.88	±9.52	0.29	0.92	±16.5
(d) Total perfusion	0.20	−5.73	±9.79	0.42	−5.21	±17.9

The trends of SO_2 and $SjvO_2$ matched during the surgery. Especially in the rewarming period, both values temporarily declined (Figs. 5 and 6), reflecting the oxygen demand-supply imbalance due to the increased metabolism of the brain and temperature effect on the hemoglobin dissociation curve. However, the $SjvO_2$ value changed between approximately 40% and 90%, while the SO_2 value changed within 50% and 80%. Thus, the SO_2 variation tended to be smaller than the $SjvO_2$ variation. In addition, the correlation and bias between the SO_2 and $SjvO_2$ also differed depending on the conditions of extracorporeal circulation, although a good correlation was observed except for perfusion for the period. These values do not necessarily match, as seen in Fig. 6, because $SjvO_2$ shows a balance between blood flow and metabolism in the whole brain, making it difficult to measure very small changes. Moreover, there is a report of increase in the shunt of arterial and venous blood flow,[10] resulting in increase of $SjVO_2$.

In contrast, the TRS may be able to perform localized tissue measurements. Thus, the SO_2 is not necessarily higher than the $SjvO_2$, due to the SO_2 showing average saturation of arterial, capillary, and venous blood, because the $SjvO_2$ shows information of the whole brain hemodynamics, including the deeper region that extracts less oxygen than the neocortex region.[12] Some studies on the correlation between NIRS SO_2 and $SjvO_2$ have shown that it almost matches,[7,28] while others have shown that it does not.[8,9,12,39] The contradiction between these results is attributable to surgery without extracorporeal circulation or differences in the method of inducing anesthesia or the temperature control conditions.

$SjvO_2$ is used as an indicator of cerebral oxygenation, where higher $SjvO_2$ shows better oxygenation conditions. However, there is a report of postoperative disturbance of higher brain functions in patients who showed high $SjvO_2$ during extracorporeal circulation.[40] Therefore, the judgment of normoxia-hypoxia by $SjvO_2$ may be insufficient, and simultaneous measurements of SO_2 by TRS can give more accurate information about the oxygenation conditions of patients.

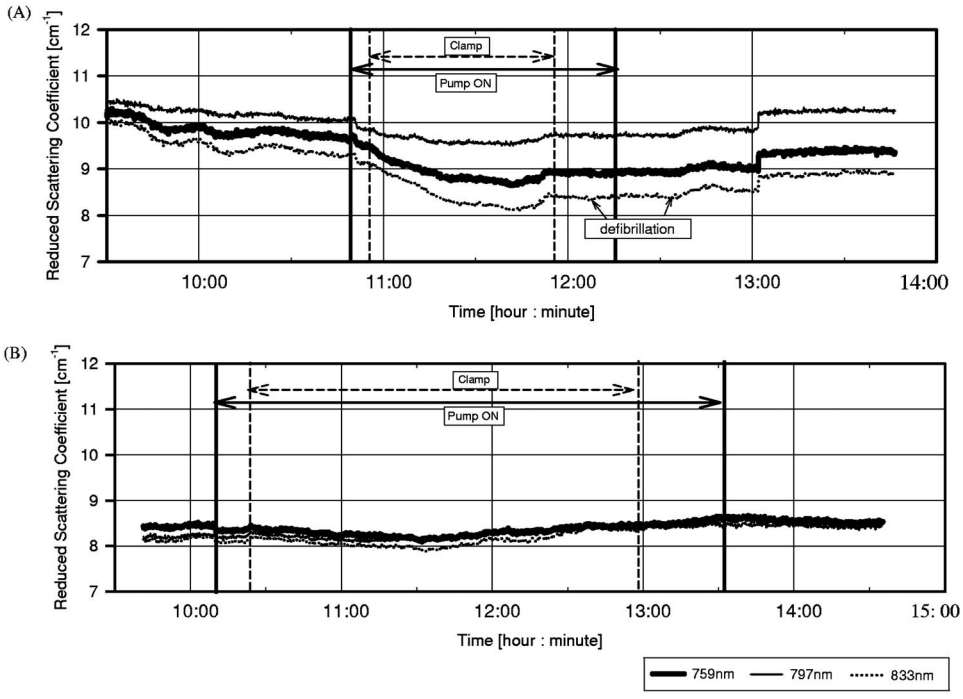

Fig. 9 (a) μ_s' decreased gradually during perfusion in one case (Case 5: M, 69Y). This trend was observed only in this case. (b) μ_s' remained unchanged in a typical case (Case 7: M, 66Y). A similar pattern was observed in the other eight patients except Case 5.

5 Conclusion

We have developed a time-resolved spectroscopy system (TRS-10) and have used it in cardiopulmonary bypass surgery as a brain oxygenation monitor. SO_2 measured by TRS paralleled fluctuations in $SjvO_2$, although these correlations depended on the perfusion conditions. Further detailed studies are necessary to clarify the relation between these values.

A good correlation was noted between tHb by TRS and Hct value (12% to 37.8%) in arterial blood ($r^2=0.63$). Intracerebral hemodynamics of patients were captured well by TRS in real time and noninvasively.

Consequently, our results indicate that TRS is a valid spectroscopic method for quantifying cerebral hemodynamics and is useful for clinical monitoring.

Clarification of the relationship between μ_s' and the pathological condition of the patient and improvement of the analytical approach[40–43] for measuring deeper regions are future challenges.

Acknowledgments

The authors would like to thank T. Hiruma and Y. Suzuki for their constant support and encouragement.

References

1. Y. Kakihana, A. Matsunaga, H. Yamada, H. Dohgomori, T. Oda, and N. Yoshimura, "Continuous, noninvasive measurement of cytochrome oxidase in cerebral cortex by near-infrared spectrophotometry during aortic arch surgery," *J. Anesth.* **10**, 221–224 (1996).
2. R. A. De Blasi, N. Almenräder, and M. Ferrari, "Brain oxygenation monitoring during cardiopulmonary bypass by near infrared spectroscopy," *Adv. Exp. Med. Biol.* **413**, 97–104 (1997).
3. J. H. Meek, C. E. Elwell, D. C. McCormick, A. D. Edwards, J. P. Townsend, A. L. Stewart, and J. S. Wyatt, "Abnormal cerebral haemodynamics in perinatally asphyxiated neonates related to outcome," *Arch. Dis. Child Fetal Neonatal Ed.* **81**(2), F110–115 (1999).
4. K. Isobe, T. Kusaka, Y. Fujikawa, M. Kondo, K. Kawada, S. Yasuda, S. Itoh, K. Hirao, and S. Onishi, "Changes in cerebral hemoglobin concentration and oxygen saturation immediately after birth in the human neonate using full-spectrum near infrared spectroscopy," *J. Biomed. Opt.* **5**(3), 283–286 (2000).
5. G. W. Roach, M. Kanchuger, C. M. Mangano, M. Newman, N. Nussmeier, R. Wolman, A. Aggarwal, K. Marschall, S. H. Graham, C. Ley, G. Ozanne, and D. T. Mangano, "Adverse cerebral outcomes after coronary bypass surgery," *N. Engl. J. Med.* **335**(25), 1857–1863 (1996).
6. M. F. Newman, J. L. Kirchner, B. Phillips-Bute, V. Gaver, H. Grocott, R. H. Jones, D. B. Mark, J. G. Reves, and J. A. Blumenthal; Neurological Outcome Research Group and the Cardiothoracic Anesthesiology Research Endeavors Investigators, "Longitudinal assessment of neurocognitive function after coronary-artery bypass surgery," *N. Engl. J. Med.* **344**(6), 395–402 (2001).
7. M. Aono, J. Sata, and T. Nishino, "Regional cerebral oxygen saturation as a monitor of cerebral oxygenation and perfusion during deep hypothermic circulatory arrest and selective cerebral perfusion," *Masui* **47**(3), 335–340 (1998).
8. P. G. Al-Rawi, P. Smielewski, and P. J. Kirkpatrick, "Preliminary evaluation of a prototype spatially resolved spectrometer," *Acta Neurochir. Suppl. (Wien)* **71**, 255–257 (1998).
9. Y. Kadoi, F. Kawahara, S. Saito, T. Morita, F. Kunimoto, F. Goto, and N. Fujita, "Effects of hypothermic and normothermic cardiopulmonary bypass on brain oxygenation," *Ann. Thorac. Surg.* **68**, 34–39 (1999).
10. A. J. McCleary, S. Gower, J. P. McGoldrick, J. Berridge, and M. J. Gough, "Does hypothermia prevent cerebral ischaemia during cardiopulmonary bypass?" *Cardiovasc. Surg.* **7**(4), 425–431 (1999).
11. M. B. Kim, D. S. Ward, C. R. Cartwright, J. Kolano, S. Chlebowski, and L. C. Henson, "Estimation of jugular venous O_2 saturation from cerebral oximetry or arterial O_2 saturation during isocapnic hypoxia," *J. Clin. Monit Comput.* **16**(3), 191–199 (2000).
12. M. Shaaban Ali, M. Harmer, R. S. Vaughan, J. A. Dunne, and I. P. Latto, "Spatially resolved spectroscopy (NIRO-300) does not agree with jugular bulb oxygen saturation in patients undergoing warm bypass surgery," *Can. J. Anaesth.* **48**(5), 497–501 (2001).
13. H. Hamada, I. Nakagawa, F. Uesugi, T. Kubo, T. Hiramatsu, T. Kai, S. Hidaka, and K. Hamaguchi, "Effects of perfusion pressure on cerebral blood flow and oxygenation during normothermic cardiopulmonary bypass," *Masui* **53**, 744–752 (2004).
14. T. A. Tortoriello, S. A. Stayer, A. R. Mott, E. D. McKenzie, C. D. Fraser, D. B. Andropoulos, and A. C. Chang, "A noninvasive estimation of mixed venous oxygen saturation using near-infrared spectroscopy by cerebral oximetry in pediatric cardiac surgery patients," *Paediatr. Anaesth.* **15**, 495–503 (2005).
15. J. W. de Vries, G. H. Visser, and P. F. Bakker, "Neuromonitoring in defibrillation threshold testing. A comparison between EEG, near-infrared spectroscopy, and jugular bulb oximetry," *J. Clin. Monit* **13**, 303–307 (1997).
16. Y. Kadoi, F. Kawahara, and N. Fujita, "Malfunctioning of cerebral function monitors in three cases of carotid endarterectomy," *Masui* **49**, 40–44 (2000).
17. T. Yasukawa, S. Endo, K. Endo, M. Mihira, K. Kimura, and A. Sari, "Continuous monitoring to detect brain ischemia during carotid endarterectomy and aortic arch replacement by near infrared spectrophotometry—a case report," *Masui* **49**, 626–629 (2000).
18. T. Ohata, Y. Sawa, S. Ohtake, M. Nishimura, N. Hirata, K. Kagisaki, S. Taketani, T. Yamaguchi, and H. Matsuda, "Evaluation of cerebral circulation during cardiopulmonary bypass using near-infrared spectroscopy," *Jpn. J. Thorac. Cardiovasc. Surg.* **46**, 603–609 (1998).
19. M. S. Patterson, J. D. Moulton, B. C. Wilson, K. W. Berndt, and J. R. Lakowicz, "Frequency-domain reflectance for the determination of the scattering and absorption properties of tissue," *Appl. Opt.* **30**, 4474–4476 (1991).
20. J. B. Fishkin and E. Gratton, "Propagation of photon-density waves in strongly scattering media containing an absorbing semi-infinite plane bounded by a straight edge," *J. Opt. Soc. Am. A* **10**, 127–140 (1993).
21. S. Fantini, M. A. Franceschini, and E. Gratton, "Semi-infinite-geometry boundary problem for light migration in highly scattering media: a frequency-domain study in the diffusion approximation," *J. Opt. Soc. Am. B* **11**(10), 2128–2138 (1994).
22. Y. Tsuchiya and T. Urakami, "Frequency domain analysis of photon migration based on the microscopic Beer-Lambert law," *Jpn. J. Appl. Phys., Part 1* **35**, 4848–4851 (1996).
23. H. Iwai, T. Urakami, M. Miwa, M. Nishizawa, and Y. Tsuchiya, "Tissue spectroscopy with a newly developed phase modulation system based on the microscopic Beer-Lambert law," *Proc. SPIE* **4250**, 482–488 (2001).
24. B. Chance, S. Nioka, J. Kent, K. McCully, M. Fountain, R. Greenfeld, and G. Holtom, "Time-resolved spectroscopy of hemoglobin and myoglobin in resting and ischemic muscle," *Anal. Biochem.* **174**, 698–707 (1988).
25. M. S. Patterson, B. Chance, and B. C. Wilson, "Time-resolved reflectance and transmittance for the noninvasive measurement of tissue optical properties," *Appl. Opt.* **28**(12), 2331–2336 (1989).
26. M. Oda, Y. Yamashita, G. Nishimura, and M. Tamura, "A simple and novel algorithm for time-resolved multiwavelength oximetry," *Phys. Med. Biol.* **41**, 551–562 (1996).
27. Y. Yamashita, M. Oda, E. Ohmae, and M. Tamura, "Continuous measurement of oxy- and deoxyhemoglobin of piglet brain by time-resolved spectroscopy," *OSA TOPS* **22**, 205–207 (1998).
28. H. M. Watzman, D. Kurth, L. M. Montenegro, J. Rome, J. M. Steven, and S. C. Nicolson, "Arterial and venous contributions to near-infrared cerebral oximetry," *Anesthesiology* **93**(4), 947–953 (2000).
29. M. Oda, Y. Yamashita, G. Nishimura, and M. Tamura, "Quantitation of absolute concentration changes in scattering media by the time-resolved microscopic Beer-Lambert law," *Adv. Exp. Med. Biol.* **345**, 861–870 (1994).
30. M. Oda, Y. Yamashita, T. Nakano, A. Suzuki, K. Shimizu, I. Hirano, F. Shimomura, E. Ohmae, T. Suzuki, and Y. Tsuchiya, "Near-infrared time-resolved spectroscopy system for tissue oxygenation monitor," *Proc. SPIE* **4160**, 204–210 (2000).

31. H. Zhang, M. Miwa, T. Urakami, Y. Yamashita, and Y. Tsuchiya, "Simple subtraction method for determining the mean path length traveled by photons in turbid media," *Jpn. J. Appl. Phys., Part 1* **37**, 700–704 (1998).
32. K. Suzuki, Y. Yamashita, K. Ohta, and B. Chance, "Quantitative measurement of optical parameters in the breast using time-resolved spectroscopy. Phantom and preliminary *in vivo* results," *Invest. Radiol.* **29**(4), 410–414 (1994).
33. C. H. Fusch, B. Scharrer, E. Hungerland, and H. Moeller, "Body water, lean body, and fat mass of healthy children as measured by deuterium oxide dilution," *Isotopes Environ. Health Stud.* **29**, 125–131 (1993).
34. B. Chance, "Time-resolved spectroscopy and imaging," *Proc. SPIE* **2389**, 122–139 (1995).
35. S. Ijichi, T. Kusaka, K. Isobe, K. Okubo, K. Kawada, M. Namba, H. Okada, T. Nishida, T. Imai, and S. Itoh, "Developmental changes of optical properties in neonates determined by near-infrared time-resolved spectroscopy," *Pediatr. Res.* **58**(3), 568–573 (2005).
36. C. Du, C. Andersen, and B. Chance, "Quantitative detection of hemoglobin saturation on piglet brain by near-infrared frequency-domain spectroscopy," *Proc. SPIE* **3194**, 55–62 (1997).
37. D. A. Boas, J. P. Culver, J. J. Stott, and A. K. Dunn, "Three-dimensional Monte Carlo code for photon migration through complex heterogeneous media including the adult human head," *Opt. Express* **10**, 159–170 (2002).
38. C. Sato, T. Yamaguchi, M. Seida, Y. Ohta, I. Yu, Y. Iguchi, M. Nemoto, and Y. Hoshi, "Intraoperative monitoring of depth-dependent hemoglobin concentration changes during carotid endarterectomy by time-resolved spectroscopy," *Appl. Opt.* **46**(14), 2785–2792 (2007).
39. Y. Shingu, K. Myojin, Y. Ishibashi, K. Ishii, M. Kawasaki, and G. Yamaura, "Real-time cerebral monitoring using multichannel near-infrared spectroscopy in total arch replacement," *Jpn. J. Thorac. Cardiovasc. Surg.* **51**(4), 154–157 (2003).
40. K. Yoshitani, M. Kawaguchi, N. Sugiyama, M. Sugiyama, S. Inoue, T. Sakamoto, K. Kitaguchi, and H. Furuya, "The association of high jugular bulb venous oxygen saturation with cognitive decline after hypothermic cardiopulmonary bypass," *Anesth. Analg. (Baltimore)* **92**(6), 1370–1376 (2001).
41. Y. Ueda, K. Ohta, Y. Yamashita, and Y. Tsuchiya, "Calculation of photon path distribution based on photon behavior analysis in a scattering medium," *Opt. Rev.* **10**(5), 444–446 (2003).
42. J. Selb, J. J. Stott, M. A. Franceschini, A. G. Sorensen, and D. A. Boas, "Improved sensitivity to cerebral hemodynamics during brain activation with a time-gated optical system: analytical model and experimental validation," *J. Biomed. Opt.* **10**(1), 011013 (2005).
43. B. Montcel, R. Chabrier, and P. Pulet, "Detection of cortical activation with time-resolved diffuse optical methods," *Appl. Opt.* **44**(10), 1942–1947 (2005).